an A-group element, and X is C or N) with a layered nature suggests they may have excellent promise as solid lubricant materials. First-generation MAX phase–based composites shafts have been successfully tested against Ni-based superalloy at 50,000 rpm from room temperature to 550°C during thermal cycling in a foil bearing rig (Gupta et al. 2007). This study further demonstrates the potential of MAX phases and their composites in different tribological applications.

Cross-References

► High-Temperature Solid Lubricating Materials
► Solid Lubricants

References

T. Akhadejdamrong, T. Aizawa, M. Yoshitake, A. Mitsuo, Feasibility study of self-lubrication by chlorine implantation. Nucl. Instrum.: Methods Phys. Res. B **207**, 45–54 (2003)

P.J. Blau, B. Dumont, D.N. Braski, Reciprocating friction and wear behavior of a ceramic-matrix graphite composite for possible use in diesel engine valve guides. Wear **225–229**, 1338–1349 (1999)

J.X. Deng, T.K. Cao, X.F. Yang, J.H. Liu, Self-lubrication of sintered ceramic tools with CaF_2 additions in dry cutting. Int. J. Mach. Tools Manuf. **46**, 957–963 (2006)

C.H. Ding, P.L. Li, G. Ran, Y.W. Tian, J.N. Zhou, Tribological property of self-lubricating PM 304 composite. Wear **262**, 575–581 (2007)

A. Gangopadhyay, S. Jahanmir, M.B. Peterson, Self-Lubricating Ceramic Matrix Composites, in *Friction and Wear of Ceramics*, ed. by S. Jahanmir (Marcel Dekker, New York, 1994), pp. 163–197

M.N. Gardos, H.-S. Hong, W.O. Winter, The effect of anion vacancies on the tribological properties of rutile (TiO_{2-x}), Part II: experimental evidence. Tribol. Trans. **22**(2), 209–220 (1990)

S. Gupta, D. Filimonov, T. Palanisamy, T. El-Raghy, M.W. Barsoum, Ta_2AlC and Cr_2AlC Ag-based composites-new solid lubricant materials for use over a wide temperature range against Ni-based superalloys and alumina. Wear **262**, 1479–1489 (2007)

C.F. Higgs III, E.Y.A. Wornyoh, An in situ mechanism for self-replenishing powder transfer films: experiments and modeling. Wear **264**, 131–138 (2008)

J.H. Ouyang, T. Murakami, S. Sasaki, Y.F. Li, Y.M. Wang, K. Umeda, Y. Zhou, High temperature tribology and solid lubrication of advanced ceramics. Key Eng. Mater. **368–372**, 1088–1091 (2008)

H.R. Pasaribu, J.W. Sloetjes, D.J. Schipper, Friction reduction by adding copper oxide into alumina and zirconia ceramics. Wear **255**, 699–707 (2003)

H.R. Pasaribu, K.M. Reuver, D.J. Schipper, S. Ran, K.W. Wiratha, A.J.A. Winnubst, D.H.A. Blank, Environmental effects on friction and wear of dry sliding zirconia and alumina ceramics doped with copper oxide. Int. J. Refract. Metals Hard Mater. **23**, 386–390 (2005)

A. Skopp, M. Woydt, Ceramic and ceramic composite materials with improved friction and wear properties. Tribol. Trans. **38**(2), 233–242 (1995)

H.E. Sliney, C. Dellacorte, The friction and wear of ceramic/ceramic and ceramic/metal combinations in sliding contact. Lubr. Eng. **50**(7), 557–576 (1994)

L. Tuchinskiy, E. Veksler, R. Loutfy, M. Williams, Tribological characteristics of Si_3N_4-based self-lubricating materials. Tribol. Trans. **43**, 603–610 (2000)

M. Woydt, M. Dogigli, P. Agatonovic, Concepts and technology development of hinge joints operated up to 1600°C in air. Tribol. Trans. **40**(4), 643–646 (1997)

Solid Lubricants, Graphene

Zhibin Lu[1], Liping Wang[2]
[1]Lanzhou Institute of Chemical Physics, Chinese Academy of Science, Lanzhou, People's Republic of China
[2]State Key Laboratory of Solid Lubrication, Lanzhou Institute of Chemical Physics, Chinese Academy of Science, Lanzhou, People's Republic of China

Synonyms

Graphene

Definition

Graphene is a single planar sheet of sp2-bonded carbon atoms. Its extended honeycomb network is the basic building block of three-dimensional graphite, one-dimensional nanotubes, and zero-dimensional fullerenes.

Scientific Fundamentals

Introduction

The rapid progress of solid lubrication technology in the past 4 decades has met the requirements of the aerospace, automotive, and other industries (Miyoshi 2001, Miyoshi et al. 2005). Solid lubricant is used when liquid lubricants do not meet the advanced requirements. In high vacuum (or space), high temperature, low temperature, radiation, clean environment, or corrosive environments, and combinations thereof, solid lubricant may be the only workable system. The materials designed for solid lubrication not only need desirable friction coefficient, but also must maintain good durability in different environments, such as high vacuum, water, air, low temperature, or dust. With the development of micro-/nano-electromechanical systems (MEMS/NEMS), the dimension match need to be considered. Specifically, the separations between MEMS/NEMS can range from 1 μm/100 nm to contact. Since experimentally discovered in 2004 (Novoselov et al. 2004), graphene has exhibited a number of intriguing properties. Theoretical and experimental tests on individual graphene nanosheets exhibit extremely high values of Young's modulus (~1,000 GPa), fracture strength (~125 GPa) (Lee et al. 2008), thermal conductivity (~3,000 Wm^{-1} K^{-1}) (Bolotin et al. 2008), mobility

of charge carriers (~200,000 $cm^2 V^{-1} s^{-1}$) (Matthew et al. 2010), and fascinating transport phenomena such as the quantum Hall effect (Castro Neto et al. 2009). Effective solid lubricants generally have a number of basic properties, such as thermal stability, low friction, low surface adherence, and outstanding elastic and mechanical properties. It is known that carbon-derived materials have outstanding lubrication properties in possession of the above desirable properties. Materials such as graphite have been widely used as lubricants for many years. Graphene is the building block of the common macroscopic solid lubricant graphite, and it is also characterized by the above-mentioned advantages. Based on these results, it can be inferred that graphene would be an effective solid lubricant.

Structure and Electronic Properties of Graphene

Graphene is a flat monolayer of carbon atoms tightly packed into a two-dimensional (2D) honeycomb lattice. Its extended honeycomb network is the basic building block of other important allotropes and can be stacked to form 3D graphite, rolled to form 1D nanotubes, and wrapped to form 0D fullerenes (Fig. 1).

Due to its true 2D structure, graphene has unique properties in many respects that are different from both usual metals and semiconductors (Castro Neto et al. 2009). It has unusual electronic excitations described in terms of Dirac fermions that move in a curved space, is an interesting mix of a semiconductor zero density of states and a metal gaplessness, and has properties of soft matter. The electrons in graphene have very long mean free paths and seem to be almost insensitive to disorder and electron–electron interactions. Graphene has also a robust but flexible structure with unusual phonon modes that do not exist in ordinary 3D solids. These properties can be easily modified with the application of electric and magnetic fields, addition of layers, control of the geometry, and, chemical doping. Furthermore, graphene can be directly and relatively easily probed by various scanning probe techniques from mesoscopic down to atomic scales, because it is not buried inside a 3D structure.

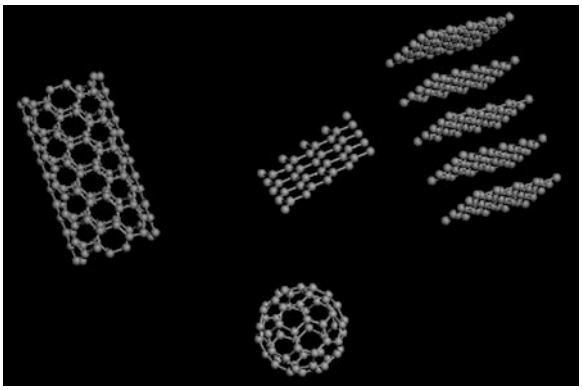

Solid Lubricants, Graphene, Fig. 1 The schematics of graphene (*middle*, *upper*), fullerene (*middle*, *lower*), carbon nanotubes (*left*), and graphite (*right*)

Elastic and Mechanical Properties of Graphene

The ideal strength is the highest achievable strength of a defect-free crystal at 0 K. Graphene is an ultrastrong material, defined by internal stress levels broadly and persistently rising up to a significant fraction of the ideal strength. Recent developments in density functional theory (DFT) methods applicable to studies of large periodic systems have become essential in addressing problems in material design and processing. The theory allows one to interpret experimental data and to determine the underlying properties of a material that is a well tested ab initio method for accurate mechanical properties. The typical steps are as follows: first, set up a supercell structure, and then apply a series of incremental tensile strains on the supercell and simultaneously relax the other stress components to zero (Poisson contraction under uniaxial tension). Then, the DFT calculated stress and Poisson's ratio varying with finite-deformation can be obtained. A representational study (Liu et al. 2007) showed that the Young's modulus $E = 1{,}050$ GPa and Poisson's ratio = 0.186. In both x and y uniaxial tensions, phonon instabilities occurred near the center of the Brillouin zone, at $\varepsilon_{xx} = 0.194$, $\sigma_{xx} = 110$ GPa, $\varepsilon_{yy} = -0.016$ and $\varepsilon_{yy} = 0.266$, $\sigma_{yy} = 121$ GPa, and $\varepsilon_{xx} = -0.027$. Both soft phonons were longitudinal elastic waves in the pulling direction, suggesting that brittle cleavage fracture would be an inherent behavior of graphene and carbon nanotubes at low temperatures.

Graphene's elastic behavior reflects the intrinsic properties of the interatomic bonding all the way up to the breaking point, because of the low defect density in the films. As suggested by Lee et al. (2008, 2009), the response of the graphene must be considered as non-linear since the stress–strain response must curve over to a maximum point that defines the intrinsic breaking stress. In the simplest model, the resulting isotropic elastic response under uniaxial extension can be expressed as

$$\sigma = E\varepsilon + D\varepsilon, \tag{1}$$

in which σ is the stress, ε the strain, E is the Young's modulus, and D is the third-order elastic modulus. There is a differential operation on both sides of the (1), thus, the maximum of the elastic stress–strain response

defines the intrinsic stress, which for this functional form is $\sigma_{\text{int}} = E^2/4D$ at strain $\varepsilon_{\text{int}} = E/2D$, so it remains only to determine E and D from the experimental results.

Graphene is a truly two-dimensional material, so its strain energy density is normalized by the area of the graphite, rather than by volume normalization. Therefore, its behavior under tensile loading is usually described by a two-dimensional strain σ_{2D}, and elastic constants E_{2D} and D_{2D}, with units of force/length. In order to obtain the corresponding three-dimensional parameters and to compare with bulk graphite and other materials, these quantities can be divided by the interlayer spacing in graphite ($h = 0.335$ nm). Since the sixfold rotation symmetry of the graphene structure, the isotropic mechanical properties are adopted. The force–displacement behavior can be approximated as (Lee et al. 2008, 2009)

$$F = \sigma_0^{2D}(\pi a)\left(\frac{\delta}{a}\right) + E^{2D}\left(q^3 a\right)\left(\frac{\delta}{a}\right)^3 \qquad (2)$$

where F is the applied force, δ is the deflection at the center point, σ_0^{2D} is the pre-tension in the film, and $q = 1.02$. Therefore, the pre-tension and the elastic modulus can be obtained by fitting the force-displacement curve to (2). For monolayer graphene, the data followed (2) until the large displacement, while the data fell significantly below the data obtained from small-displacement curve fitting for the displacement of more than 50 nm of bilayer graphene. The measured mean values of moduli (E_{2D}) for monolayer, bilayer, and trilayer graphene were 342, 698, and 986 N/m, respectively (Lee et al. 2008, 2009). These correspond to Young's moduli of $E = 1.02$, 1.04, and 0.98 TPa, assuming 0.335 nm as the thickness of one layer. Within experimental error, the Young's moduli of monolayer, bilayer, and trilayer graphene are all identical and equal to the value for bulk graphite.

The fracture strength of graphene was measured by loading the membranes to the breaking point, but the force required to break the membranes depended strongly on the tip radius due to the extreme stress concentration at the tip, which can be described as (Lee et al. 2008, 2009):

$$\sigma_m^{2D} = \left(\frac{FE^{2D}}{4\pi R}\right)^{\frac{1}{2}} \qquad (3)$$

where σ_m^{2D} is the maximum stress at the central point of the film, F is the breaking force, and R is the tip radius. Equation (3) yielded an average breaking strength of 55 N/m for monolayer graphene. However, because the model ignored non-linear elasticity, this value overestimated the strength. To extract the true breaking strain, Lee et al. performed a series of finite element simulations, using non-linear stress–strain behavior given by (1). For monolayer films, this value was $D = 680$ N/m, yielding a two-dimensional ultimate strength of 42 N/m, which corresponded to a strength of 130 GPa in the bulk limit.

To provide a good estimate for bilayer and trilayer membranes, the measured strength of monolayer graphene, together with the tip radius used in each experiment, was used to scale the multilayer results. The estimated strength, which represented an upper bound of the true strength, decreased with the thickness, from 126 GPa for bilayers to 101 GPa for trilayer graphene (Lee et al. 2008, 2009).

Frictional Properties of Graghene

Generally, the microtribological behavior was evaluated using an AFM. The friction forces are proportional to the applied loads obeying Amonton's law

$$F_L \cdot \ddot{y} = \mu F_N + F_0 \qquad (4)$$

where μ is the friction coefficient, F_L is the friction force, F_N is the normal load, and F_0 is the friction force at an external load of zero. Actual friction forces are difficult to obtain, and F_L is expressed as voltage signals; correspondingly, the real friction coefficients ($\mu = \partial F_L/\partial F_N$) could not be feasibly calculated. However, a relative friction coefficient (RFC), which is the slope of the force curve, can be obtained. Therefore, for a given AFM probe, the RFCs for various samples can be compared with each other.

The results of micro-scale frictional experiments performed in an ambient environment (Lee et al. 2009) showed that, independent of scan speed (from 1 to 10 mm/s) and the applied load (from 0.1 to 2 nN), the friction force decreases monotonically with sample thickness, and converges to that of bulk graphite as the number of layers increase above 5.

Atomic-scale frictional experiments tested in a dry nitrogen purged chamber by Lee et al. showed that the energy dissipation decreased monotonically as the number of graphene layers increases, and approaches that of bulk graphite, consistent with the micrometer-scale measurements in ambient conditions. In addition, the adhesion force between the tip and graphene flakes with different numbers of layers showed that there was virtually no difference between different thicknesses. Furthermore, measured friction on suspended graphene membranes showed that there is no difference between suspended and supported graphene.

After ruling out substrate effects and influence of adhesion, Lee et al. concluded that the layer-dependence of friction appears to be governed by dissipation mechanisms taking place at the tip-graphene interface.

Understanding the fundamental origin of friction is one of the pressing challenges with the miniaturization of moving components in many commercial products, including computer disk heads and the microelectromechanical systems that trigger the airbags in cars. At the core of the problem is an identification of the mechanisms that convert kinetic energy of sliding contacts into heat. By reducing the thickness of the solid lubricant graphite to the most extreme limits, single and double atomic layers of graphene grown epitaxially on SiC, Filleter et al.demonstrated that there was a significant difference in friction between single and bilayer graphene films. And this difference was related to dramatic reduction in electron–phonon coupling in the bilayer as revealed by angle-resolved photoemission spectroscopy. Filleter et al. explored friction and dissipation in epitaxial graphene films, revealing that bilayer graphene as a lubricant outperforms even graphite due to reduced adhesion (Filleter et al. 2009).

Tribological Properties of Reduced Graphene Oxide Sheets

The characteristic properties of graphene include outstanding thermal conductivity, novel electronic properties, and excellent mechanical behavior and make it the ideal candidate for the basic building block of MEMS/NEMS. However, the difficulty of obtaining a stable graphene structure on device surfaces has hindered its potential in MEMS/NEMS because of the lack of function groups in graphene. Because of abundance of oxygenous groups in graphene oxide (GO) molecules, it is advisable to assemble the reduced GO (RGO) microstructure on a substrate by performing thermal treatment.

Following the above, Ou et al. (2010) have assembled the stable RGO sheets onto the surface of a silicon wafer by a multi-step method. First, a 3-aminopropyl triethoxysilane self-assembled monolayer (coded APTES-SAM) was prepared on the silicon wafer via a self-assembly process. Then GO was grafted onto a silicon substrate covered with APTES-SAM through chemical reactions between the oxygenous and amine groups. Finally, the RGO was obtained by annealing the formed GO, in which the obtained sample was coded APTES-RGO. WCA measurement is a simple, useful, and sensitive tool for gaining insight into surface chemical components. Ou et al. have shown that the hydroxylated silicon wafer and APTES-GO were hydrophilic with WCA of ~0 and 40.2, respectively. Correspondingly, high adhesive forces of ~190/~140 nN were generated between the AFM tip and the samples of hydroxylated silicon substrate/APTES-GO. Once APTES-GO was reduced, WCA increases to 85.5, and adhesive force decreased to ~100 nN, exhibiting good adhesion resistance.

The microtribological properties evaluated with an AFM by Ou et al. show that the hydroxylated silicon wafer possessed the highest friction and RFC. Both APTES-GO and APTES-RGO reduced friction. APTES-RGO exhibited the best lubricity, which could be assigned to the smallest adhesive force compared with the hydroxylated silicon wafer and APTES-GO as well as the lowest surface energy (reflected by the highest WCA of 85.5).

The macrotribological behavior of APTES-SAM, graphite, APTES-GO, APTES-RGO, and RGO on bare Si substrate at an applied load of 0.1 N, and APTES-RGO at an applied load of 0.2 N, have been tested on a ball-on-plate macrotribometer by Ou et al. Test results show that APTES-SAM displayed poor tribological properties characterized by high friction and very short antiwear life under the testing conditions of 0.1 N and 1 Hz. Once GO was assembled, the sample exhibited improved tribological properties characterized by a reduced friction coefficient (~0.25) and a lengthened antiwear life (~1,600 s). Upon thermal reduction, antiwear life increased further to >10,800 s and the reduced friction coefficient remained unchanged.

The friction coefficient of the APTES-RGO was a little lower than that of graphite plate (about 0.28) and lower than the friction coefficient of carbon nanotube (CNT) (about 0.3–0.5) tested by a similar ball-on-disk tribometer.

Key Application

Tribological Application of Composite Coating and Composites Reinforced with Graphene

Because of the effects of their improved mechanical properties and unique structure, carbon-derived materials such as fullerene and carbon nanotubes can be used to fabricate composites and coatings with excellent tribological performance attributed to their excellent mechanical properties and the unique topological structure of carbon-derived materials.

Graphene is considered an excellent candidate for developing functional and structure-reinforced composites because of its remarkable mechanical properties, such as exceptionally high elastic modulus, large elastic strain, and fracture strain sustaining capability. Incorporation of graphene into polymer matrices remarkably improves the mechanical properties of the materials (Wang et al. 2009, Zhao et al. 2010). It is expected that graphene-reinforced

composites and coatings will have extensive tribological application. The introduction of graphene can improve the mechanical properties of composites and coatings. In addition, the formation of carbon film can reduce the friction and wear rate.

Graphene Platelets as a Lubricant Additive

Lin et al. (2011) demonstrated that the graphene platelets modified by stearic and oleic acids could be added as lubricant additive to stably disperse in oil. The wear resistance and load-carrying capacity of the lubricating oil were greatly improved with the addition of the modified graphene platelets at an optimal content of 0.075 wt.%. During the friction process, the wear rate and the friction coefficients of both the base oil and the oil with the modified graphene platelets increased remarkably. However, the wear rates and the friction coefficient of the oil with modified graphene platelets were relatively steady throughout the test. Moreover, the friction coefficient of the oil with modified graphene platelets was much lower than that of the base oil and oil with modified graphene platelets. And the modified graphene platelets have better tribological properties than the modified graphene platelets when used as additives.

Graphene/RGO as Lubricant on MEMS/NEMS

A graphene/RGO sheet, which has a thickness of several nanometers, matched with the separations between MEMS/NEMS, will be an ideal choice as lubricant film on a nanoscale due to not only the excellent electronic and mechanical properties but also because of potential friction reduction and antistiction performance.

Cross-References

► Graphite Solid Lubrication Materials
► Solid Lubricants

References

K.I. Bolotin, K.J. Sikes, Z. Jiang, M. Klima, G. Fudenberg, J. Hone, P. Kim, Ultrahigh electron mobility in suspended graphene. Solid State Commun. **146**, 351–355 (2008)

A.H. Castro Neto, F. Guinea, N.M.R. Peres, K.S. Novoselov, A.K. Geim, The electronic properties of graphene. Rev. Mod. Phys. **81**, 109–162 (2009)

T. Filleter, J.L. McChesney, A. Bostwick, E. Rotenberg, K.V. Emtsev, Th Seyller, K. Horn, R. Bennewitz, Friction and dissipation in epitaxial graphene films. Phys. Rev. Lett. **102**, 086102 (2009)

C. Lee, X. Wei, J.W. Kysar, J. Hone, Measurement of the elastic properties and intrinsic strength of monolayer graphene. Science **321**, 385–388 (2008)

C. Lee, X. Wei, Q. Li, R. Carpick, J.W. Kysar, J. Hone, Elastic and frictional properties of graphene. Phys. Status Solidi B **246**, 2562–2567 (2009)

J. Lin, L. Wang, G. Chen, Modification of graphene platelets and their tribological properties as a lubricant additive. Tribol. Lett. **41**, 209–215 (2011)

F. Liu, P. Ming, J. Li, *Ab initio* calculation of ideal strength and phonon instability of graphene under tension. Phys. Rev. B **76**, 064120 (2007)

J.A. Matthew, C.T. Vincent, B.K. Richard, Honeycomb carbon: a review of graphene. Chem. Rev. **110**, 132–145 (2010)

K. Miyoshi, *Solid Lubrication Fundamentals and Applications* (Marcel Dekker, New York, 2001)

K. Miyoshi, K.W. Street Jr., R.L. Vander Wal, A. Rodney, A. Sayir, Solid lubrication by multiwalled carbon nanotubes in air and in vacuum. Tribol. Lett. **19**, 191–201 (2005)

K.S. Novoselov, A.K. Geim, S.V. Morozov, D. Jiang, Y. Zhang, S.V. Dubonos, I.V. Grigorieva, A.A. Firsov, Electric field effect in atomically thin carbon films. Science **306**, 666–669 (2004)

J. Ou, J. Wang, S. Liu, B. Mu, J. Ren, H. Wang, S. Yang, Tribology study of reduced graphene oxide sheets on silicon substrate synthesized via covalent assembly. Langmuir **26**, 15830–15836 (2010)

D.W. Wang, F. Li, J.P. Zhao, W.C. Ren, Z.G. Chen, J. Tan, Z.S. Wu, I. Gentle, G.Q. Lu, H.M. Cheng, Fabrication of graphene/polyaniline composite paper via in situ anodic electropolymerization for high-performance flexible electrode. ACS Nano **3**, 1745–1752 (2009)

X. Zhao, Q. Zhang, D. Chen, P. Lu, Enhanced mechanical properties of graphene-based poly (vinyl alcohol) composites. Macromolecules **43**, 2357–2363 (2010)

Solid Lubricants, Layered-Hexagonal Transition Metal Dichalcogenides

Tomas Polcar
Department of Control Engineering, Faculty of Electrical Engineering, Czech Technical University in Prague, Prague, Czech Republic

Definition

Transition metal dichalcogenides (TMD) are among the best alternatives as solid lubricants for tribological applications, particularly in dry and vacuum environments. Their excellent lubricating properties are based on the extreme crystal anisotropy; under ideal conditions (very dense material deposited and tested in ultra-high vacuum) they can be considered as "frictionless," i.e., with friction coefficient as low as 0.001. Pure TMD are sensitive to the presence of water vapor, exhibiting high friction coefficient. For tribological purposes, TMD are prepared in the form of powder, burnished films, thin films, inorganic fullerene-like particles, or nanotubes.